Simulation of Magnetically Dispersed Arc Plasma

2012 Plasma Sci. Technol. 14 118

(http://iopscience.iop.org/1009-0630/14/2/07)

Simulation of Magnetically Dispersed Arc Plasma*

BAI Bing (白冰), ZHA Jun (查俊), ZHANG Xiaoning (张晓宁),
WANG Cheng (王城), XIA Weidong (夏维东)

Department of Thermal Science and Energy Engineering, University of Science and Technology, Hefei 230027, China

Abstract Magnetically dispersed arc plasma [1] exhibits typically dispersed uniform arc column as well as diffusive cathode root [1,2] and diffusive anode root. In this paper magnetically dispersed arc plasma coupled with solid cathode is numerically simulated by the simplified cathode sheath model of LOWKE [3]. The numerical simulation results in argon show that the maximum value of arc root current density on the cathode surface is 3.5×10^7 A/m^2, and the maximum value of energy flux on the cathode surface is 3×10^7 J/m^2, both values are less than the average values of a contracted arc, respectively.

Keywords: magnetically dispersed arc plasma, diffusive arc root, cathode, numerical simulation

PACS: *52.25.Kn, 52.80.Mg*

DOI: 10.1088/1009-0630/14/2/07

1 Introduction

Traditional arc plasma is of concentrated energy and its parameters are inhomogeneous. The magnetically dispersed arc plasma in LADAPS [1] (Large Area Dispersed Arc Plasma Source) is characterized by uniform density and energy distribution. Besides the dispersed arc column, the magnetic dispersed arc plasma shows a diffusive arc root at the cathode as well as at the anode, as shown in Fig. 1 [4].

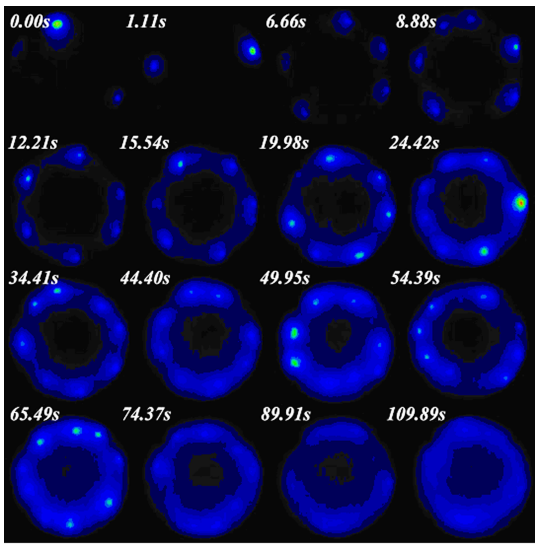

Fig.1 Diffusive process of arc root on the end of cathode in LADAPS

In Fig. 1, there is only one arc root at the cathode surface while arc ignites at 0.00 s. As time proceeds, the cathode root splits into multiple roots, finally at 109.89 s, there is no conspicuous cathode arc root indicated by the highlight point but a diffused arc root around the cathode.

Although LI [5] has simulated dispersed arc plasma in LADAPS with a simplified cathode model, in which the cathode temperature and the current density are fixed, it is obviously that LI's results are inconsistent with the experimental results, especially at the cathode arc root and the nearby region. Hence we should take the cathode into consideration with emphasis laid on the arc roots diffusion.

There have been several papers presenting models for the near cathodes region. BENILOV [6] takes the near cathode region as sheath and ionized layer. The electron density is obtained by solving Poisson equation and Boltzmann equation; and in the space charge ionized layer, multicomponent hydrodynamic equations are employed to get the space-charge distribution. In HSU's paper [7], the cathode region is divided into two subzones: the ionization zone and the space-charge zone. The ionization zone is used to account for the generation of ions and electrons using electron Boltzmann equation, and the latter is used for explaining the sheath formation.

The above mentioned models only contra pose the near cathode region. LOWKE et al. [3] proposed a simplified model of arc and cathode. The method of calculation omits any account of the space-charge sheath at the cathode. The electron density and thus the electrical conductivity within the cathode sheath region are evaluated by assuming ambipolar diffusion. Current density values are derived from the current continuity equation. M. TANAKA et al. [8] employed this model to calculate molten pool formation and thermal plasma

*supported by National Natural Science Foundation of China (Nos. 50876101, 11035005)

with metal vapor in gas tungsten arc welding, and the calculation result appears to be consistent with the experiments.

In this paper, magnetically dispersed arc plasma coupled with cathode is simulated with LOWKE's model to analyze the behavior of the arc roots such as the current density distribution and the energy flux on the cathode surface.

2 Simulation model

Besides the heat conduction to the cathode surface, simulation of arc plasma coupled with cathode should include the special energy transfer processes occurring at the surface, which are cooling processes due to the thermionic emission and radiation, heating process due to ion current. Heating by radiation from the plasma is neglected. For cathode, the additional energy flux F.

$$F = -\varepsilon\alpha {T_\mathrm{c}}^4 - |j_\mathrm{e}|\phi_\mathrm{c} + |j_\mathrm{i}|V_\mathrm{i}, \tag{1}$$

ε is the emissivity of the surface, T_c is the surface temperature, α is the Stefan-Boltzmann constant, j_e is the electron current density, ϕ_c is the work function which depends on the cathode material, j_i is the ion current density which is assumed to be $j_\mathrm{i} = |j| - |j_\mathrm{R}|$ at the cathode surface, and V_i is the ionization potential of the plasma, where $j = j_\mathrm{e} - j_\mathrm{i}$ is the current density at the surface of the cathode obtained from Poisson's equation. j_R is the theoretical thermionic emission current density given by the following Richardson equation:

$$|j_\mathrm{R}| = AT_\mathrm{c}^2 \exp\frac{-\phi_\mathrm{c} e}{k_\mathrm{B} T_\mathrm{c}}, \tag{2}$$

where A is the thermionic emission constant for the surface of the cathode, e is the electronic charge, k_B is Boltzmann constant. If $|j_\mathrm{R}|$ is greater than $|j|$, we take j_i to be zero.

The temperature of the near cathode region is about the value of melting point, the non-equilibrium effects can make the near cathode region highly conductive. Therefore, we introduce an effective electric conductivity to express Ohm's Law in this region.

The electron continuity equation is:

$$\bigtriangledown \cdot (D_\mathrm{A} \bigtriangledown n_\mathrm{e}) = \gamma(n_\mathrm{e}^2 - n_\mathrm{eq}^2), \tag{3}$$

where: D_A is the ambipolar diffusion coefficient for the local temperature given by $\frac{2kT\mu_\mathrm{i}}{e}$. μ_i is the ion mobility defined by Langevin mobility. n_e is the electron density and $\gamma = 1.1 \times 10^{-12} n_\mathrm{e} T^{-4.5}$ cm^3/s is the electron-ion recombination coefficient, n_eq is the equilibrium plasma value of electron density corresponding to the local plasma temperature.

Then the effective electrical conductivity of near cathode region σ_eff is derived as:

$$\sigma_\mathrm{eff} = \frac{n_\mathrm{e} e}{n_0/(n_\mathrm{T}\mu_\mathrm{e}) + (2en_\mathrm{e}n_\mathrm{eq})/(n_\mathrm{T}\sigma)}, \tag{4}$$

where n_0 is the equilibrium neutral particle density, μ_e is the electron mobility $\mu_\mathrm{e} = \frac{e}{m_\mathrm{e}\nu}$, ν is the collision frequency of the electron $\nu = \frac{\lambda_\mathrm{e}}{v_\mathrm{t}}$, v_t is the electron velocity defined by the local temperature, λ_e is the electron mean free path, $n_\mathrm{T} = n_0 + n_\mathrm{e} + n_\mathrm{eq}$ is the total particle density.

Fig. 2 shows the two-dimensional cylindrical coordinate diagram of the coaxial plasma generator. A-C-D-E-F-G-H is the computational domain. A-C is the symmetry axis. A-H-J-B is the graphite cathode region. G-F-E is the anode surface. G-H is the gas inlet, where there was an imposed argon gas flow around the cathode. And E-D-C is the external environment with argon at 1 atmosphere pressure. A uniform axial magnetic field is present in the computational domain.

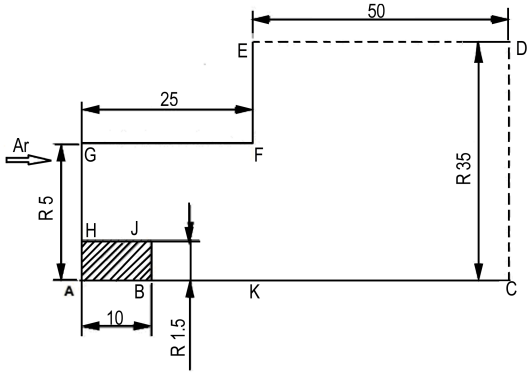

Fig.2 Computational domain (mm)

Table 1. Boundary condition

-	P(atm)	V(m/s)	T(K)	Φ	A	n_e
A-C	$\frac{\partial P}{\partial n}=0$	$\frac{\partial V}{\partial n}=0$	$\frac{\partial T}{\partial n}=0$	$\frac{\partial \Phi}{\partial n}=0$	$\frac{\partial A}{\partial n}=0$	$\frac{\partial n_\mathrm{e}}{\partial n}=0$
H-J-B	-	$\frac{\partial V}{\partial n}=0$	F	coupled	coupled	$\frac{j_R}{ev_\mathrm{t}}$
A-H	-	-	300	$\frac{\partial \Phi}{\partial n}=j_{in}$	$\frac{\partial A}{\partial n}=0$	-
H-G	1	1.5	300	$\frac{\partial \Phi}{\partial n}=0$	$\frac{\partial A}{\partial n}=0$	$\frac{\partial n_\mathrm{e}}{\partial n}=0$
G-F-E	-	$\frac{\partial V}{\partial n}=0$	1000	$\Phi=0$	$\frac{\partial A}{\partial n}=0$	-
E-D-C	1	0	300	$\frac{\partial \Phi}{\partial n}=0$	$\frac{\partial A}{\partial n}=0$	-

The plasma flow here is assumed to be turbulent and steady, optically thin and in local thermodynamic equilibrium. The MHD equations can be found in Ref. [9].

3 Simulation results

As shown in Fig. 3, the point of peak temperature (14990.7 K) in the plasma is about 2 mm in front of the end of cathode at the symmetry axis, not near the edge of the end. In the plasma column region, from 15 mm to 21 mm, the temperature distribution is uniform, and the temperature gradient is small.

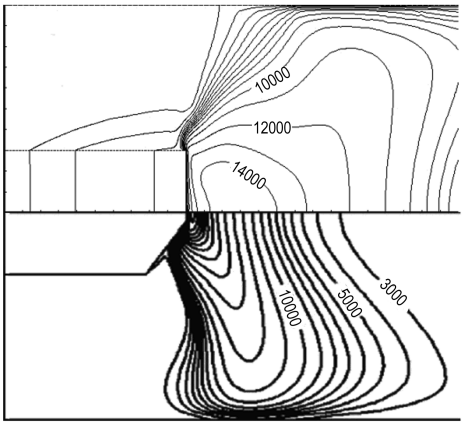

Fig.3 Plasma temperature distribution

In Fig. 4, (From Figs. 4∼6: the cathode surface is placed along the x axis, from H (x=0) to J (x=10 mm) to B (x=11.5 mm)) the maximum temperature on the cathode surface is at the edge of the end (at"J" in Fig. 2), which is 3427.7 K, less than the sublimation temperature of graphite. In view of the position of the cathode ablation zone in experiment and the luminance of the diffused cathode arc root in Fig. 1, we can infer that the peak temperature region is around the end which is in agreement with the calculation result. Except for the surface approaching the maximum temperature point, the distribution of the temperature is smooth. From 8 mm to 11.5 mm, the surface temperature is above 3000 K. The maximum temperature of the plasma is not near the maximum temperature of the cathode surface.

Fig. 5 is the distribution of the energy flux at the cathode surface. Thermionic emission (ec) and ion heating (ih) play dominant roles. The energy fluxes of the two processes are greater than 5×10^7 J/m^2, and the energy flux of the radiation (rad) and the heat conduction (heat) are less than 1×10^7 J/m^2. From 9.75 mm, the energy flux of heat conduction increases sharply. Because the plasma temperature in root region is much higher than the plasma temperature in non-root region, and the difference between temperatures is large. (The values at point J in Fig. 2 is insignificant which is a singular point in the simulation)

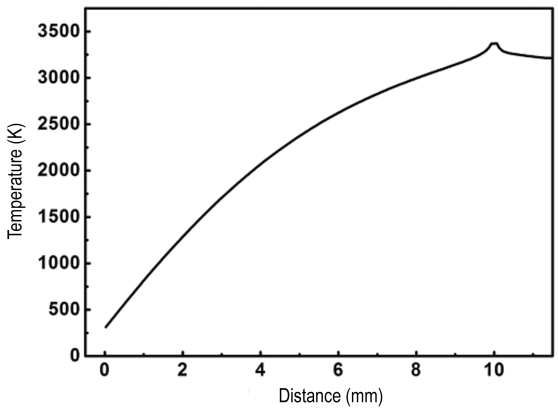

Fig.4 Cathode surface temperature

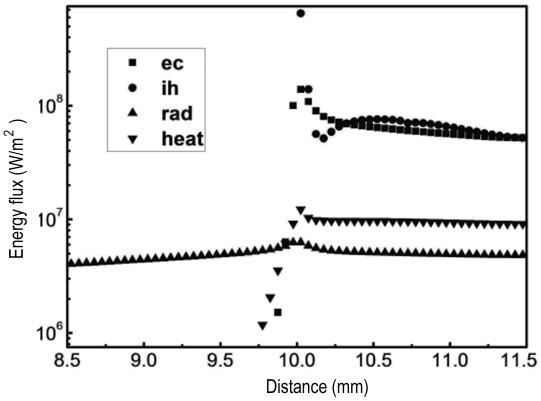

Fig.5 Energy flux distribution at the cathode surface

Fig. 6 shows the current distribution on the cathode tip and the side wall of the cathode. With the singular point (from 9.6 mm to 10 mm) eliminated, the peak current density is 3.5×10^7 A/m^2, and the average current density is 1.85×10^7 A/m^2. The current density of a contracted arc root is about 1.1×10^8 A/m^2, which is greater than the diffused current density. The profile of the current j is greater than 9.75×10^6 A/m^2 from 9.75 mm to 11.5 mm, which means that the top of the cathode is filled with current even though current also exists at the side of the cathode. According to current density, we conclude that the cathode root is diffused under the effect of axial magnetic field.

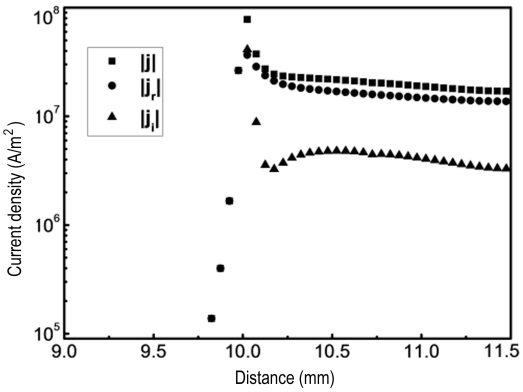

Fig.6 The current density distribution on the cathode tip and the side wall of the cathode

4 Conclusions

The temperature of diffused root arc plasma is lower than the temperature of the contracted root arc plasma. The peak temperature of the diffused root arc plasma is 10.7% less than that of a contracted root arc plasma, which is about 16800 K [10].

The maximum current density of the diffused arc root is less than that of a contracted root, in which the diffusion plays a positive role in protecting the cathode.

The major process of the energy transfer is thermionic emission and ion heating, which are both significantly larger than the radiation and the heat conduction.

References

1 Xia Weidong, Li Lincun, Zhao Yuhan, et al. 2006, Applied Physics Letters, 88: 211501

2 Li Lin cun, Chen Quan, Zhou Heling, et al. 2008, IEEE Transactions on Plasma Science, 36: 1080

3 Lowke J, Morrow R, Haidar J. 1997, J. Phys. D: Appl. Phys., 30: 2033

4 Xia Weidong, Zhou Heling, Zhou Zhipeng, et al. 2008, IEEE Transactions on Plasma Science, 36: 1048

5 Li Lincun, Xia Weidong. 2008, Japanese Journal of Applied Physics, 47: P273

6 Benilov M S, Marotta A. 1995, J. Phys. D: Appl. Phys., 28: 1869

7 Hsu K C, Pfender E. 1983, J. Appl. Phys., 54: 3818

8 Tanaka M, Yamamoto K, Tashiro S, et al. 2010, J. Phys. D: Appl. Phys., 43: 434009

9 Chen Xi. 2009, Heat Transfer and Flow of Thermal Plasma. Science Press, Beijing, p.333 (in Chinese)

10 Li lincun, Xia Weidong. 2008, Plasma Science and Technology, 10: 328

(Manuscript received 6 August 2011)
(Manuscript accepted 16 December 2011)
E-mail address of BAI Bing: baibing@mail.ustc.edu.cn